Figure S1

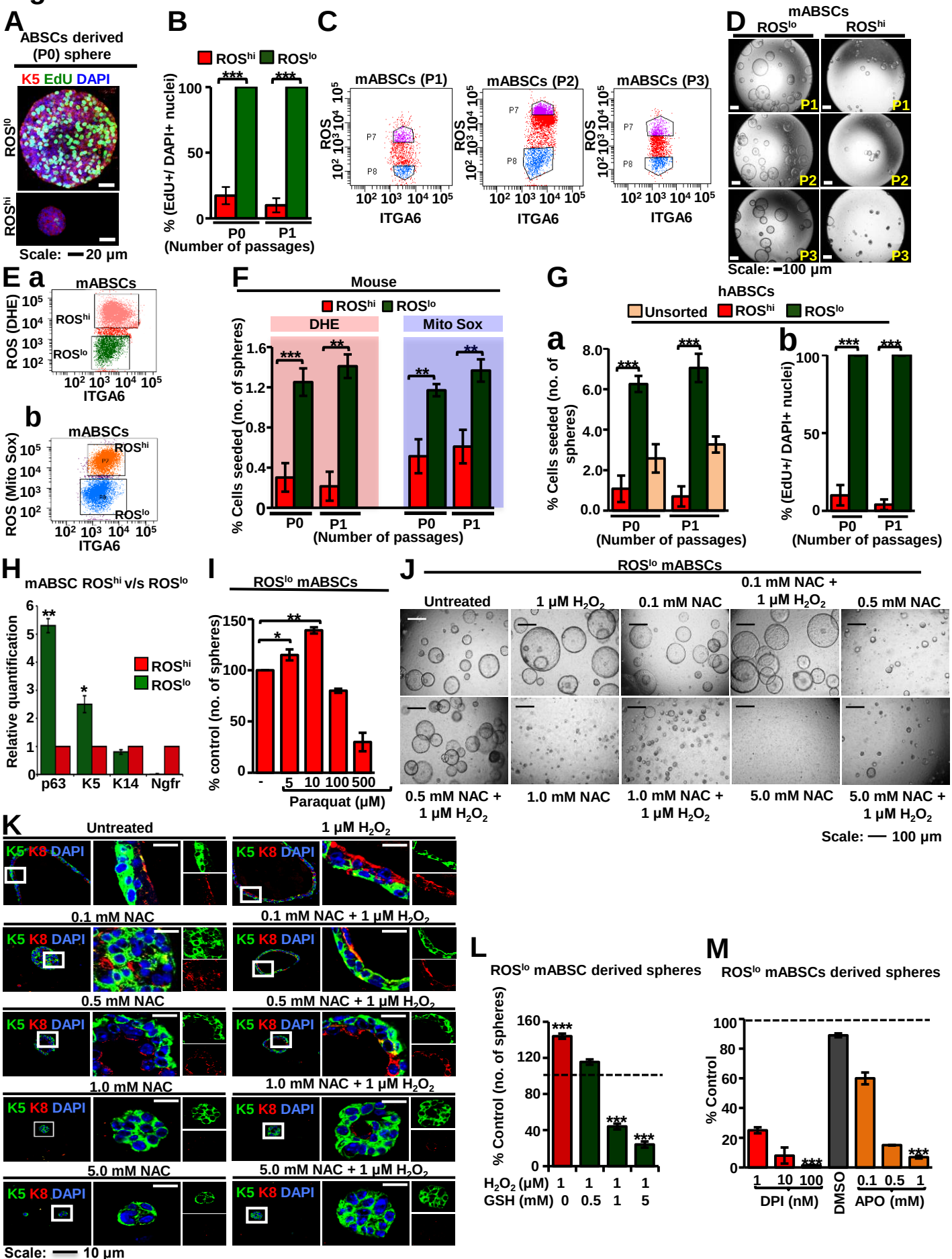
A
ABSCs derived (P0) sphere
K5 EdU DAPI
ROSlo
ROShi
Scale: 20 µm
B
ROShi ROSlo
% (EdU+/ DAPI+ nuclei)
P0 P1
(Number of passages)
C
mABSCs (P1)
mABSCs (P2)
mABSCs (P3)
ROS
ITGA6
P7
P8
D
mABSCs
ROSlo ROShi
P1 P2 P3
Scale: 100 µm
E a
mABSCs
ROS (DHE)
ROShi
ROSlo
ITGA6
b
ROS (Mito Sox)
F
Mouse
DHE
Mito Sox
% Cells seeded (no. of spheres)
(Number of passages)
G
hABSCs
Unsorted ROShi ROSlo
a
% Cells seeded (no. of spheres)
b
% (EdU+/ DAPI+ nuclei)
H
mABSC ROShi v/s ROSlo
Relative quantification
p63 K5 K14 Ngfr
I
ROSlo mABSCs
% control (no. of spheres)
Paraquat (µM)
J
ROSlo mABSCs
Untreated
1 µM H2O2
0.1 mM NAC
0.1 mM NAC + 1 µM H2O2
0.5 mM NAC
0.5 mM NAC + 1 µM H2O2
1.0 mM NAC
1.0 mM NAC + 1 µM H2O2
5.0 mM NAC
5.0 mM NAC + 1 µM H2O2
Scale: 100 µm
K
Untreated
1 µM H2O2
0.1 mM NAC
0.1 mM NAC + 1 µM H2O2
0.5 mM NAC
0.5 mM NAC + 1 µM H2O2
1.0 mM NAC
1.0 mM NAC + 1 µM H2O2
5.0 mM NAC
5.0 mM NAC + 1 µM H2O2
K5 K8 DAPI
Scale: 10 µm
L
ROSlo mABSC derived spheres
% Control (no. of spheres)
H2O2 (µM) 1 1 1 1
GSH (mM) 0 0.5 1 5
M
ROSlo mABSCs derived spheres
% Control
1 10 100
DPI (nM)
DMSO
0.1 0.5 1
APO (mM)

Figure S2

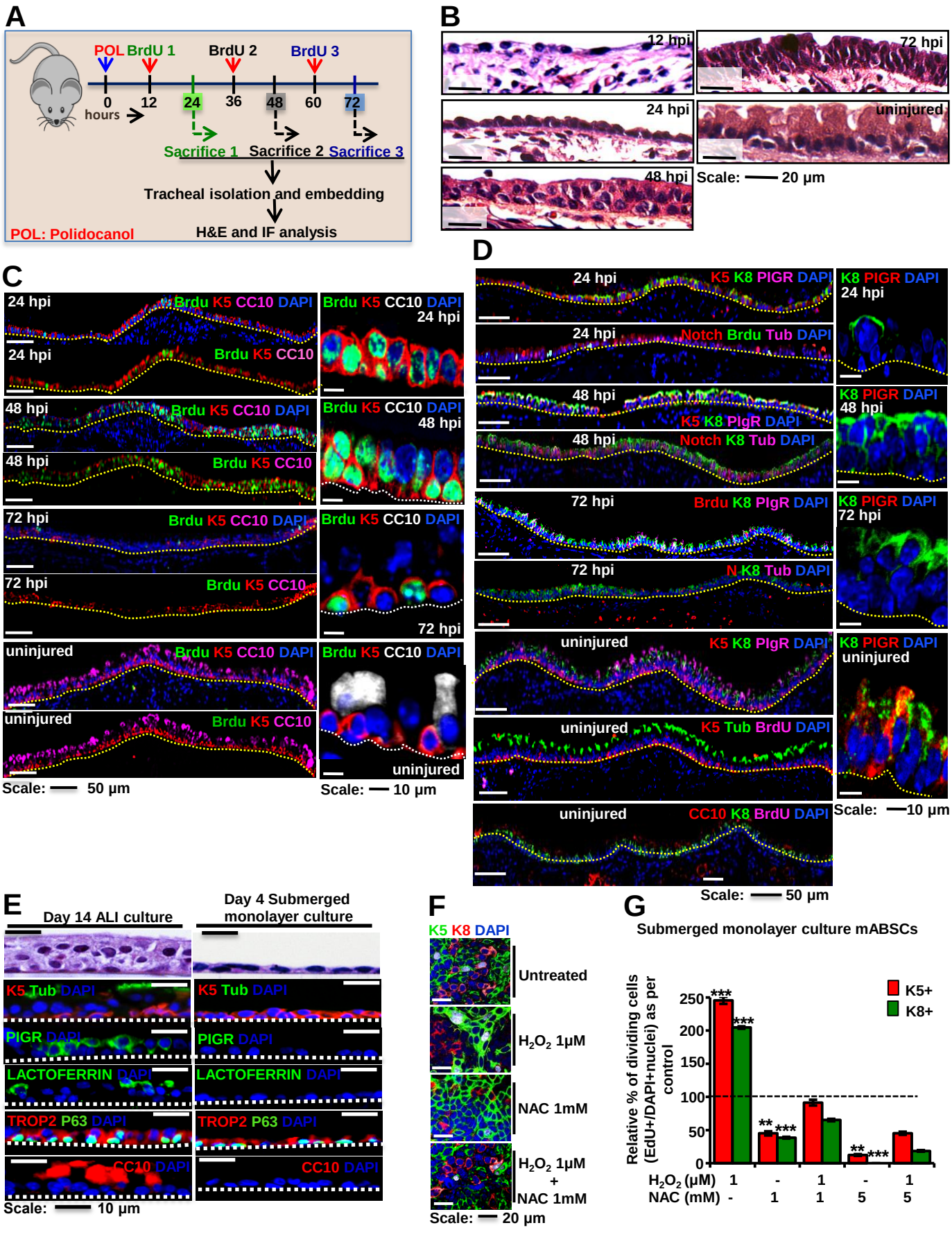
A
POL BrdU 1
BrdU 2
BrdU 3
0
12
24
36
48
60
72
hours
Sacrifice 1
Sacrifice 2
Sacrifice 3
Tracheal isolation and embedding
H&E and IF analysis
POL: Polidocanol
B
12 hpi
72 hpi
24 hpi
uninjured
48 hpi
Scale: 20 µm
C
24 hpi
Brdu K5 CC10 DAPI
Brdu K5 CC10
48 hpi
72 hpi
uninjured
Scale: 50 µm
Scale: 10 µm
D
K5 K8 PIGR DAPI
K8 PIGR DAPI
Notch Brdu Tub DAPI
K5 K8 PIgR DAPI
Notch K8 Tub DAPI
Brdu K8 PIgR DAPI
N K8 Tub DAPI
K5 K8 PIgR DAPI
K5 Tub BrdU DAPI
CC10 K8 BrdU DAPI
Scale: 10 µm
Scale: 50 µm
E
Day 14 ALI culture
Day 4 Submerged monolayer culture
K5 Tub DAPI
PIGR DAPI
LACTOFERRIN DAPI
TROP2 P63 DAPI
CC10 DAPI
Scale: 10 µm
F
K5 K8 DAPI
Untreated
H2O2 1µM
NAC 1mM
H2O2 1µM + NAC 1mM
Scale: 20 µm
G
Submerged monolayer culture mABSCs
Relative % of dividing cells (EdU+/DAPI+nuclei) as per control
K5+
K8+
H2O2 (µM) 1 - 1 - 1
NAC (mM) - 1 1 5 5

Figure S3

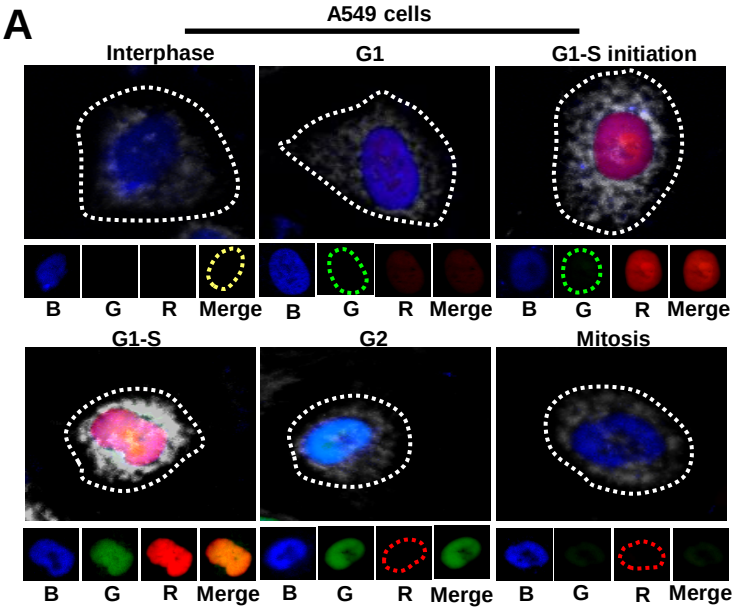
A
A549 cells
Interphase
G1
G1-S initiation
B G R Merge B G R Merge B G R Merge
G1-S
G2
Mitosis
B G R Merge B G R Merge B G R Merge

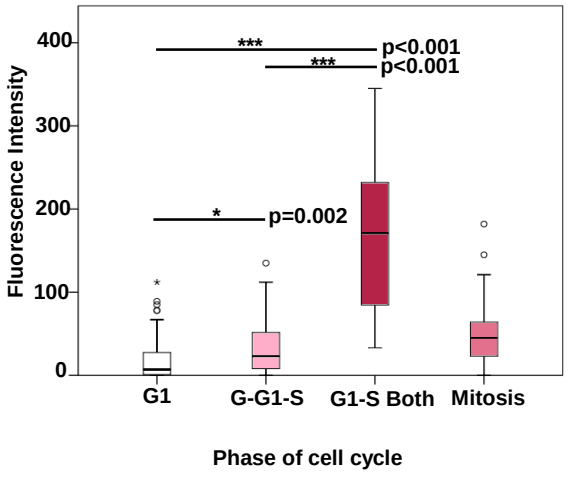
B
Fluorescence Intensity
400
300
200
100
0
***
p<0.001
***
p<0.001
*
p=0.002
G1
G-G1-S
G1-S Both
Mitosis
Phase of cell cycle

Figure S4

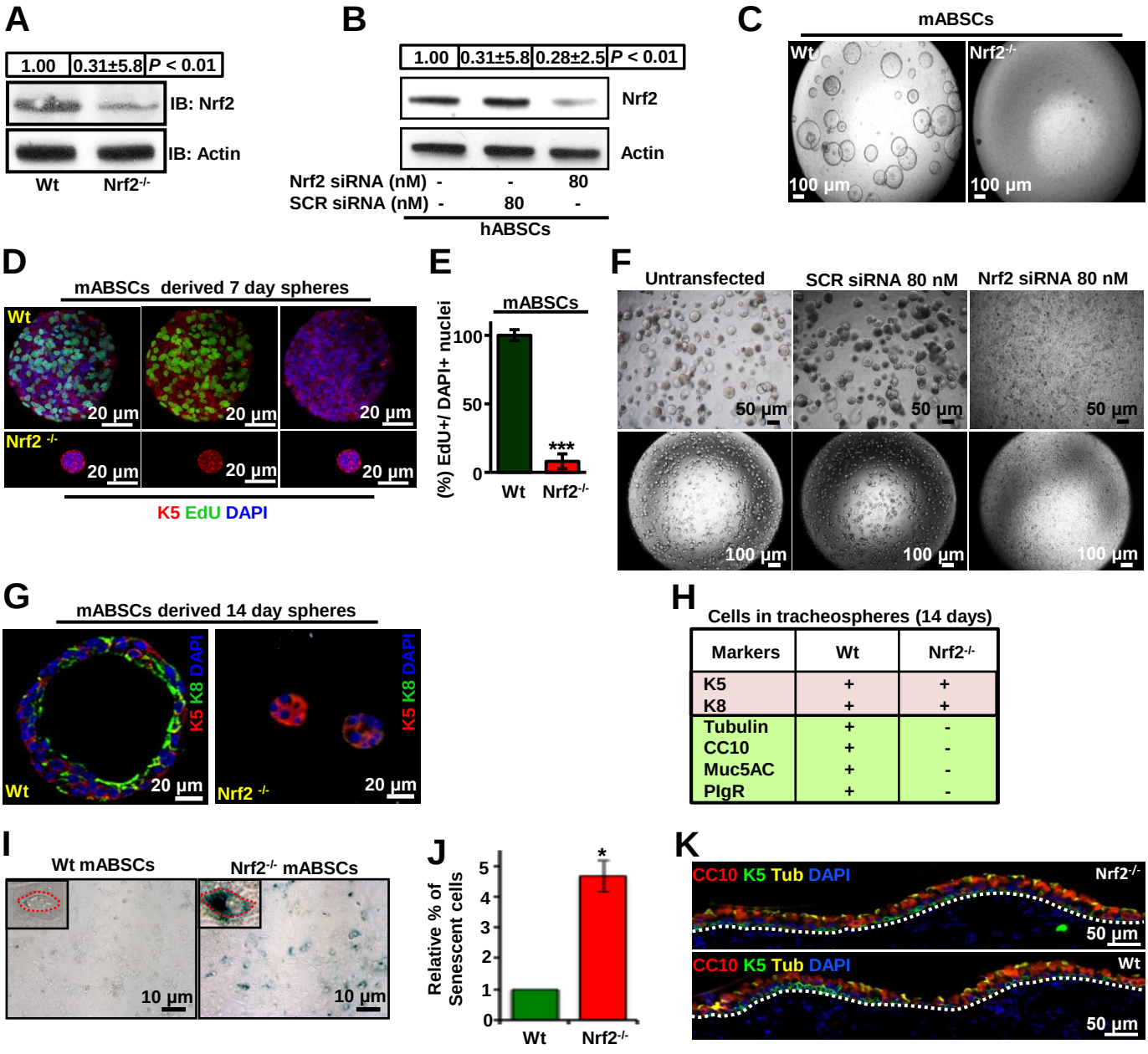
A
1.00
0.31±5.8
P < 0.01
IB: Nrf2
IB: Actin
Wt
Nrf2-/-
B
1.00
0.31±5.8
0.28±2.5
P < 0.01
Nrf2
Actin
Nrf2 siRNA (nM) - - 80
SCR siRNA (nM) - 80 -
hABSCs
C
mABSCs
Wt
Nrf2-/-
100 µm
100 µm
D
mABSCs derived 7 day spheres
Wt
Nrf2 -/-
20 µm
K5 EdU DAPI
E
mABSCs
(%) EdU+/ DAPI+ nuclei
100
50
0
***
Wt
Nrf2-/-
F
Untransfected
SCR siRNA 80 nM
Nrf2 siRNA 80 nM
50 µm
100 µm
G
mABSCs derived 14 day spheres
K5 K8 DAPI
Wt
Nrf2 -/-
20 µm
H
Cells in tracheospheres (14 days)
Markers | Wt | Nrf2-/-
K5 | + | +
K8 | + | +
Tubulin | + | -
CC10 | + | -
Muc5AC | + | -
PlgR | + | -
I
Wt mABSCs
Nrf2-/- mABSCs
10 µm
J
Relative % of Senescent cells
5
4
3
2
1
0
*
Wt
Nrf2-/-
K
CC10 K5 Tub DAPI
Nrf2-/-
50 µm
CC10 K5 Tub DAPI
Wt
50 µm

Figure S5

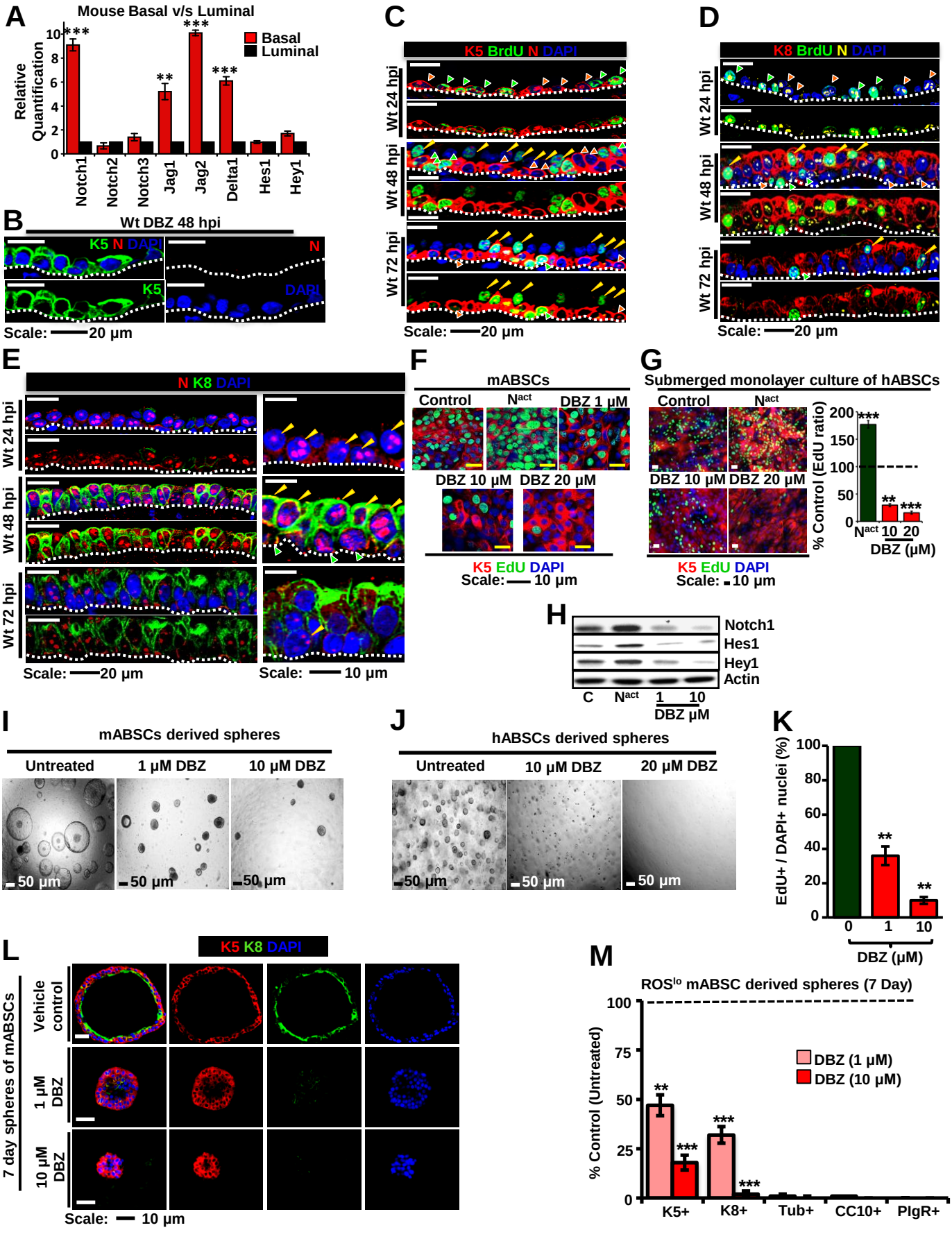
A
Mouse Basal v/s Luminal
Basal
Luminal
Relative Quantification
Notch1
Notch2
Notch3
Jag1
Jag2
Delta1
Hes1
Hey1
B
Wt DBZ 48 hpi
K5 N DAPI
N
K5
DAPI
Scale: 20 µm
C
K5 BrdU N DAPI
Wt 24 hpi
Wt 48 hpi
Wt 72 hpi
Scale: 20 µm
D
K8 BrdU N DAPI
Wt 24 hpi
Wt 48 hpi
Wt 72 hpi
Scale: 20 µm
E
N K8 DAPI
Wt 24 hpi
Wt 48 hpi
Wt 72 hpi
Scale: 20 µm
Scale: 10 µm
F
mABSCs
Control
Nact
DBZ 1 µM
DBZ 10 µM
DBZ 20 µM
K5 EdU DAPI
Scale: 10 µm
G
Submerged monolayer culture of hABSCs
Control
Nact
DBZ 10 µM
DBZ 20 µM
K5 EdU DAPI
Scale: 10 µm
% Control (EdU ratio)
Nact
DBZ (µM)
H
Notch1
Hes1
Hey1
Actin
C
Nact
DBZ µM
I
mABSCs derived spheres
Untreated
1 µM DBZ
10 µM DBZ
50 µm
J
hABSCs derived spheres
Untreated
10 µM DBZ
20 µM DBZ
50 µm
K
EdU+ / DAPI+ nuclei (%)
DBZ (µM)
L
K5 K8 DAPI
7 day spheres of mABSCs
Vehicle control
1 µM DBZ
10 µM DBZ
Scale: 10 µm
M
ROSlo mABSC derived spheres (7 Day)
% Control (Untreated)
DBZ (1 µM)
DBZ (10 µM)
K5+
K8+
Tub+
CC10+
PIgR+

Figure S6

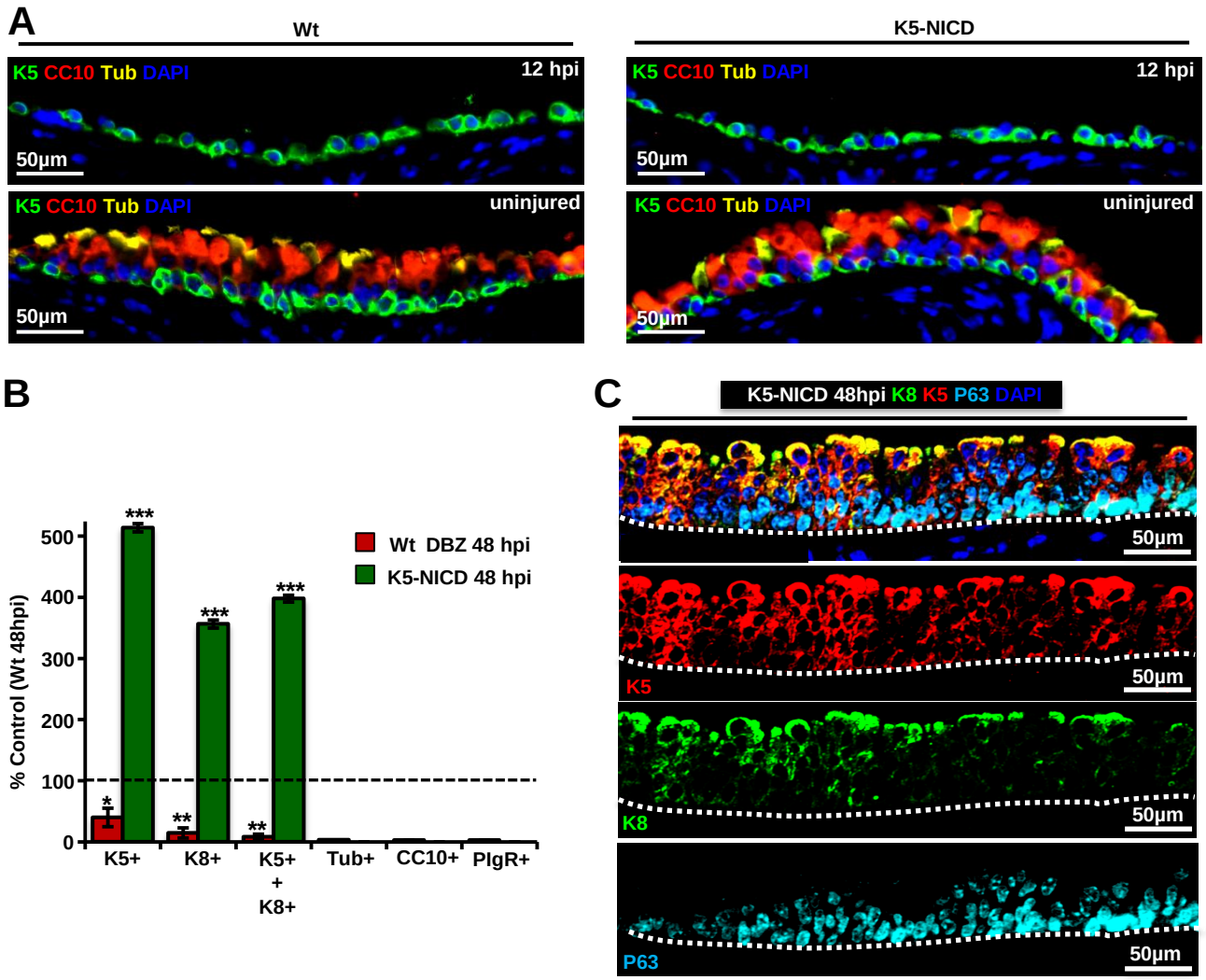
A
Wt
K5-NICD
K5 CC10 Tub DAPI
12 hpi
uninjured
50µm
B
% Control (Wt 48hpi)
Wt DBZ 48 hpi
K5-NICD 48 hpi
K5+
K8+
K5+ + K8+
Tub+
CC10+
PIgR+
C
K5-NICD 48hpi K8 K5 P63 DAPI
K5
K8
P63

Figure S7

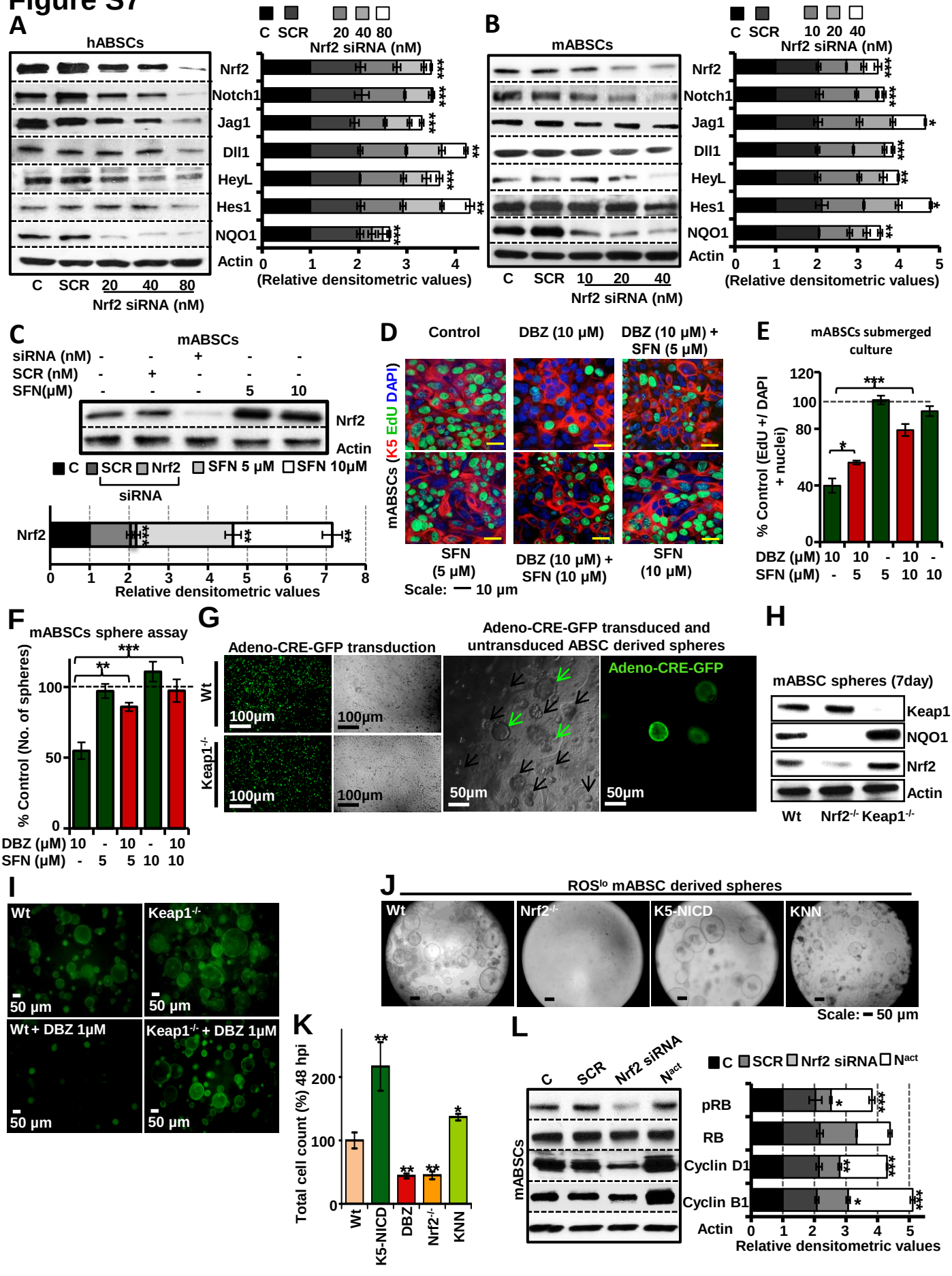
A
hABSCs
C SCR 20 40 80
Nrf2 siRNA (nM)
Nrf2
Notch1
Jag1
Dll1
HeyL
Hes1
NQO1
Actin
(Relative densitometric values)
B
mABSCs
C SCR 10 20 40
Nrf2 siRNA (nM)
C
mABSCs
siRNA (nM)
SCR (nM)
SFN(μM)
C SCR Nrf2 SFN 5 μM SFN 10μM
siRNA
Relative densitometric values
D
Control
DBZ (10 μM)
DBZ (10 μM) + SFN (5 μM)
mABSCs (K5 EdU DAPI)
SFN (5 μM)
DBZ (10 μM) + SFN (10 μM)
SFN (10 μM)
Scale: 10 μm
E
mABSCs submerged culture
% Control (EdU +/ DAPI + nuclei)
DBZ (μM)
SFN (μM)
F
mABSCs sphere assay
% Control (No. of spheres)
DBZ (μM)
SFN (μM)
G
Adeno-CRE-GFP transduction
Adeno-CRE-GFP transduced and untransduced ABSC derived spheres
Wt
Keap1-/-
100μm
50μm
Adeno-CRE-GFP
H
mABSC spheres (7day)
Keap1
NQO1
Nrf2
Actin
Wt Nrf2-/- Keap1-/-
I
Wt
Keap1-/-
Wt + DBZ 1μM
Keap1-/- + DBZ 1μM
50 μm
J
ROSlo mABSC derived spheres
Wt
Nrf2-/-
K5-NICD
KNN
Scale: 50 μm
K
Total cell count (%) 48 hpi
Wt
K5-NICD
DBZ
Nrf2-/-
KNN
L
C SCR Nrf2 siRNA Nact
mABSCs
C SCR Nrf2 siRNA Nact
pRB
RB
Cyclin D1
Cyclin B1
Actin
Relative densitometric values

Supplemental Figure Legends

Figure S1. ROS flux to The "sweet spot" Results in Maximal Self-renewal and Proliferation of ABSCs, Related to Figure 1

(A) Confocal 3D merged images of representative spheres derived from ROS^{hi} and ROS^{lo} mABSCs. Proliferation measured by EdU staining of tracheospheres cultured for 7 days. **(B)** Quantification of proliferation for two successive serial passages (P0, P1). **(C)** Airway epithelium was isolated and sorted into ABSCs ($Trop2^{+}$ and $ITGA6^{+}$) and luminal cells ($Trop2^{+}$ and $ITGA6^{-}$). Sorted ABSCs were also characterized by immunostaining with other cytoplasmic markers Trp-63 (p63) and keratin5 (K5) (data not shown). The respective populations were further separated on the basis of ROS into ROS^{hi} and ROS^{lo} (top 20% and bottom 20%) populations. Individual populations were seeded for tracheosphere cultures. The majority of spheres were formed from the ROS^{lo} ABSCs (P0). First generation spheres from ROS^{lo} ABSCs, P0 were again analyzed for their ROS status after 14 days in culture. Initially ROS^{lo} ABSCs changed their ROS status and gave rise to both ROS^{hi} and ROS^{lo} populations and were sorted again and seeded to form second generation tracheospheres (P1). The same strategy was used to examine clonal tracheosphere forming potential up to the fourth generation (P3). FACS plots 14 days old ROS^{lo} ABSC derived tracheospheres formed after 14 days in culture from originally ROS^{lo} sorted ABSCs were sorted again for ROS into ROS^{hi} and ROS^{lo} ($Trop2^{+}ITGA6^{+}$) populations and placed again into the tracheosphere culture and this was repeated for 3 passages (P1-P3). **(D)** Bright field images of tracheosphere cultures at 14 days from ROS^{hi} and ROS^{lo} mABSCs showing clonal proliferation and sphere formation efficiency for passages (P1-P3).
(E) mABSCs were also FACS sorted into ROS^{hi} and ROS^{lo} populations using two different ROS sensitive dyes, **(a)** DHE, (a superoxide detector) and **(b)** Mito SOX (a mitochondrial superoxide detector). **(F)** Both DHE and Mito SOX were used for sorting ROS^{hi} and ROS^{lo} populations and these populations were placed in the tracheosphere assay and serially passaged. **(Ga)** hABSCs were also subjected to secondary sorting based on their ROS levels (H_2DCFDA) and placed in tracheosphere cultures (P1) and quantified by counting the number of spheres generated as a percentage of seeded cells from ROS^{hi}, ROS^{lo} and unsorted cell populations. **(Gb)** Proliferation of ROS^{lo} as compared to ROS^{hi} cell populations in tracheospheres was measured by the number of EdU+/DAPI+ cells in the P0 and P1 generations. Data are presented as mean ± SEM, (n = 5). **(H)** Real time qPCR analysis of p63, K5, K14 and Ngfr (ABSC markers) gene expression in freshly FACS purified ROS^{hi} versus ROS^{lo} ABSCs. The graph shows mean values ± SEM, (n = 6). **(I)** The effect of increasing the endogenous levels of ROS with paraquat in the tracheosphere cultures. Data are presented as mean ± SEM, (n = 6). **(J)** Representative images of ROS^{lo} mABSC derived tracheospheres treated with different concentrations of NAC in the presence of a fixed concentration of H_2O_2 (1μM). The quantification is shown in Figure 1E. **(K)** Representative immunofluorescence images of tracheospheres showing expression of ABSC marker (K5) and early progenitor (EP) marker (K8) with varying concentrations of H_2O_2 and NAC. **(L)** Reduced Glutathione (L-GSH) was added to the ROS^{lo} ABSC tracheosphere cultures treated with H_2O_2 (1μM) for its anti-oxidant effects. Data are presented as mean ± SEM, (n = 3). **(M)** mABSC cultures were treated with different concentrations of diphenylene iodonium (DPI) and apocynin (APO) and analyzed for the number of tracheospheres formed. Data are presented as mean ± SEM, (n = 5). All data are presented as mean ± SEM. Significance was calculated by two-tailed, paired Student's *t*- test. * $P < 0.05$, ** $P < 0.01$, *** $P < 0.001$.

Figure S2. ABSC Repair Models, Related to Figure 2

(A) Schematic illustration of experimental strategy for polidocanol injury and airway repair *in vivo* model. **(B)** Hematoxylin and Eosin (H&E) counter staining of Wt injured tracheas after 12, 24, 48 and 72 hrs post injury (hpi) with polidocanol in comparision to Wt uninjured trachea. **(C)** Representative immunofluorescence (IF) images of Wt injured airway epithelium stained for proliferation marker (BrdU), ABSC (K5), and Club cells (CC10) at different time points after injury. Right panel shows enlarged images. **(D)** Representative IF images of 24, 48, 72 hpi and uninjured airway epithelium stained for ABSC (K5), EP (K8), serous (PIgR), and ciliated cells (acetylated β-tubulin). Notch activation is measured by staining with a primary anti-Notch intracellular domain (NICD) specific antibody. Right panel shows enlarged sections showing K8 and PIgR localization at different time points. **(E)** Characterization of submerged monolayer ABSC culture for expression of basal and differentiation markers. Freshly sorted mABSCs were cultured on collagen-coated transwells for 4 days in submerged conditions (media in upper and lower chambers) or for 14 days in the air liquid interface (ALI) culture. The cells were stained for ABSC markers (K5 and P63) and the differentiation markers (Tub, PIgR, Lactoferrin, Trop2, CC10). **(F)** The relative proliferation of K5 (K5+EdU+) and K8 (K8+EdU+) expressing cells in the submerged monolayer cultures with NAC and H_2O_2 treatments. **(G)** Quantification of relative proliferation of K5 and K8 expressing cells in the submerged monolayer cultures of mABSC with NAC and H_2O_2 treatments. All data are presented as mean ± SEM. Significance was calculated by two-tailed, paired Student's *t*- test. * $P < 0.05$, ** $P < 0.01$, *** $P < 0.001$.

Figure S3. Correlation Between Phase of Cell Cycle and ROS Levels, Related to Figure 3

(A) A549 lung cancer cells were transfected with cell cycle specific FUCCI markers and ROS levels at different phases of cell cycle progression were studied. G1 (nucleus red, marked by Cdt1-RFP), G1-S initiation (nucleus reddish orange, Cdt1-RFP and Geminin-GFP), G1-S (nucleus orange, Cdt-RFP and Geminin GFP) and Mitosis (nucleus green, Geminin GFP), (R: red, G: green, Merge: R+G). ROS status was studied using CellROX Deep Red dye (white dots) and nuclei were stained with Hoechst (B: blue). 3D merged representative images of cells (n=300) at different stages of cell cycle are shown along with their corresponding ROS status. **(B)** To investigate a difference in the distribution of the fluorescence intensity by phase of cell cycle in A549 cells a Kruskal-Wallis (KW) test was run. After the significant overall KW test ($p<0.001$), follow-up Wilcoxon rank-sum tests were utilized to assess which phases were different. This post-hoc analysis yielded statistically significant differences as shown.

Figure S4. Loss of Nrf2 Expression Reduces ABSC Proliferation, Related to Figure 4

(A) Expression analysis of Nrf2 by western-immunoblotting (WB) of mABSCs isolated from Wt and $Nrf2^{-/-}$ mouse tracheas. Actin is used as loading control. Relative densitometric values are shown. **(B)** hABSCs were transfected with Nrf2 specific siRNA or scrambled (SCR) siRNA control and Nrf2 expression was analyzed by WB. Actin was used as a loading control. Relative densitometric values are shown above the blots. **(C)** Representative images of tracheosphere cultures from Wt and $Nrf2^{-/-}$ mice. **(D)** 3D merge representative confocal images of EdU incorporation in tracheospheres from Wt and $Nrf2^{-/-}$ mice cultured for 7 days. **(E)** Bar graph representing the percentage of EdU positive cells in Wt and $Nrf2^{-/-}$ tracheospheres, considering Wt as 100%. Data are presented as mean ± SEM, (n = 6). **(F)** Representative images of hABSC tracheosphere cultures transfected with Nrf2 siRNA or SCR siRNA. Data show Nrf2 knockdown inhibits hABSCs proliferation and the phenotype is similar to ROS^{hi} hABSCs sorted and cultured on the basis of ROS

(Figure 1D). Quantification is shown in Figure 4C. **(G)** Representative sections through tracheospheres from Wt and Nrf2$^{-/-}$ mABSCs at day 14 of culture with immunostaining for ABSC (K5) and EP (K8) marker. (**H)** No markers of airway epithelial differentiation were observed in the Nrf2$^{-/-}$ tracheospheres by immunostaining, but were present (though not abundantly) in Wt tracheospheres after 14 days of culture. **(I)** Representative image from Wt and Nrf2$^{-/-}$ mABSCs stained for senescence-associated β-galactosidase (SA-βGal) activity. **(J)** Quantification of the amount of SA-βGal positive cells in Wt and Nrf2$^{-/-}$ mABSCs relative to Wt mABSCs. (**K)** Immunofluorescence image of Wt and Nrf2$^{-/-}$ uninjured tracheal epithelium showing ABSC marker K5 in green and the main differentiated cells (Club and ciliated cells marked by CC10 and acetylated β-tubulin respectively). The airway epithelia are indistinguishable in Wt and Nrf2$^{-/-}$ trachea. All data are presented as mean ± SEM. Significance was calculated by two-tailed, paired Student's *t*- test. * $P < 0.05$, ** $P < 0.01$, *** $P < 0.001$.

Figure S5. Gene Expression Analysis of Notch Signaling Molecules in Mouse Airway Epithelium, Related to Figure 5

(A) qRT-PCR validation of Notch pathway components that are differentially expressed in basal/stem and luminal/differentiated populations in mouse airway. **(B)** Negative control for NICD immunofluorescence (IF) staining. Representative immunofluorescence image of Wt airway treated with DBZ at 48 hpi with polidocanol showing K5 immunostaining and a lack of NICD immunostaining. **(C)** Representative immunofluorescence images of 24, 48, 72 hpi airway epithelium stained for ABSC marker (K5), activated Notch (NICD), and BrdU incorporation. Dotted white line shows basement membrane, K5 is localized to the cytoskeleton of the cell surface (Figure 1A) and NICD is localized to the nucleus (Figure 5B). Green arrowhead shows K5+,N+,BrdU+ cells, orange arrowhead shows K5+,N+,BrdU- cells, while yellow arrowhead shows K5-,N+,BrdU+ cells. **(D, E)** Dual NICD and K8 immunofluorescence staining at 24, 48 and 72 hpi. Yellow arrowheads show NICD localization in K8+,BrdU+ cells (dividing EPs). **(F)** mABSCs were cultured in a submerged monolayer and Notch levels were modulated by treating cells with DBZ or a Notch1 constitutively activating plasmid (N^{act}). ABSC proliferation was determined by calculating the ratio of EdU+ cells divided by the total number of cells (DAPI+) and compared with control. All cells in the culture represent mABSCs as demonstrated by the K5 immunostaining. **(G)** hABSCs were cultured in a submerged monolayer and Notch levels were modulated by treating cells with DBZ or a Notch1 constitutively activating plasmid (N^{act}). Representative IF images of proliferating stem cells expressing K5 (red) and proliferation marker EdU (green). Graph represents the effect of Notch modulation on hABSC proliferation. **(H)** Representative western-immunoblots of mABSCs after Notch activation (N^{act}) and inhibition (DBZ treatments) for the expression of Notch pathway components. **(I)** Representative images of mABSC derived tracheosphere cultures treated with DBZ for 14 days at different concentrations. **(J)** Representative images of hABSC derived tracheosphere cultures treated with DBZ at different concentrations. **(K)** Proliferation was quantified by counting the percent of EdU+/DAPI+ nuclei in the spheres. Data are presented as mean ± SEM, (n = 5). **(L)** Representative images of K5+ and K8+ cells in mABSC derived tracheospheres treated with DBZ. **(M)** Quantification of K5+ (ABSCs), K8+ (EPs), and Tub+, CC10+, PIgR+ (differentiated cells) after DBZ treatment in mABSC derived tracheospheres. Data are presented as mean ± SEM, (n = 5). All data are presented as mean ± SEM. Significance was calculated by two-tailed, paired Student's *t*-test. * $P < 0.05$, ** $P < 0.01$, *** $P < 0.001$.

Figure S6. Characterization of K5NICD Transgenic Mouse Airway Injury Model, Related to Figure 6

(A) Immunofluorescence images of Wt and K5-NICD mice tracheal epithelium at 12 hpi and in the uninjured state for K5, CC10 and Tubulin. **(B)** Quantification of K5+ and K8+ and differentiated cells (Tub+, CC10+, PIgR+) in Wt (vehicle treated), Wt DBZ treated and K5-NICD (Ru486 induced) mice at 48 hpi. Data are presented as mean ± SEM, (n = 9), and significance was calculated by two-tailed, paired Student's *t*- test. * $P < 0.05$, ** $P < 0.01$, *** $P < 0.001$. **(C)** Immunofluorescence staining of K5-NICD (Ru486 induced) mice tracheal epithelium after 48 hpi for K5, K8 and p63 expression.

Figure S7. Nrf2-Notch signaling for ABSC Proliferation, Related to Figure 7

(A, B) Nrf2 expression was knocked down in mouse and human ABSCs with siRNAs and the effect on the protein levels of Notch1, Jagged1, Delta1, HeyL, Hes1 and NQO1 were examined by western-immunoblotting. C: control and SCR: Scrambled siRNA. Right panels show densitometric data from the blots (n=3). **(C)** Nrf2 expression was examined by western-immunoblotting after treating mABSCs with Nrf2 siRNA or sulforaphane. Relative densitometry values are shown in the bottom panel. Data are presented as mean ± SEM, (n = 3). **(D)** Representative immunofluorescence images of proliferating mABSCs in submerged monolayer cultures stained with K5 and EdU. Proliferation was quantified after treatment with pharmacologic agents that modulate Notch and Nrf2, DBZ (Notch inhibition), sulforaphane (SFN) (Nrf2 activation) and DBZ with SFN treatment. **(E)** Quantification of proliferating mABSCs under conditions of Notch inhibition (DBZ treated) and Nrf2 activation (sulforaphane (SFN) treated) in submerged monolayer cultures. **(F)** Quantification of the number of spheres generated from mABSCs under conditions of Notch inhibition (DBZ) and Nrf2 activation (SFN) in the tracheosphere assay. **(G)** Left panel represents GFP-Adeno Cre transduction efficiency in Wt and $Keap1^{-/-}$ mice derived ABSCs. Right panel represents tracheospheres derived from transduced cells. A mixture of transduced and untransduced cells yields green and non-green spheres, where the non-green spheres serves as internal controls. **(H)** Representative western blots of mABSCs from $Keap1^{fl/fl}$ mice and $Nrf2^{-/-}$ mice for Nrf2, NQO1 and Keap1 expression. **(I)** Adenoviral-Cre-GFP was transduced into FACS purified $Keap1^{fl/fl}$ ABSCs in order to inhibit Keap1 expression and activate Nrf2 (GFP+ spheres) and untransfected ABSCs from the same culture were used as endogenous controls (non-GFP+ spheres). Tracheospheres were treated with DBZ to inhibit Notch activation. **(J)** Tracheosphere phenotypes from Wt (vehicle treated), $Nrf2^{-/-}$(vehicle treated), K5NICD (Ru486 induced) and K5-NICD/ $Nrf2^{-/-}$ (KNN) (Ru486 induced) transgenic mice. **(K)** Quantification of total cell counts in the repairing airway epithelium at 48 hpi in Wt, Nrf2-/-, K5-NICD, DBZ treated Wt and KNN mice. Data are presented as mean ± SEM;(n = 8). **(L)** Western blots demonstrate the effect of Nrf2 inhibition and Notch activation on cell cycle related proteins pRB, RB, cyclin D1 and cyclin B1 (n=3). Values are as mean ± SEM. * $P < 0.05$, ** $P < 0.01$ and *** $P < 0.001$.

Supplemental Tables:

Table S1. Genotyping primers for mice, Related to Experimental Procedures

Nrf2 Exon	GCCTGAGAGCTGTAGGCCC	Nrf2 Intron	GGAATGGAAAATAGCTCCTGC
LacZ	GGGTTTTCCCAGTCACGAC		
Cre F	ACCTGAAGATGTTCGCGATT	Cre R	CGAACCTGGTCGAAATCAGT
$Notch^{mut}$ F	AAAGTCGCTCTGAGTTGTTAT	$Notch^{mut}$ R	GAAAGACCGCGAAGAGTTTG
$Notch^{wt}$ F	CCAAAGTCGCTCTGAGTTGTTATC	$Notch^{wt}$ R	GAGCGGGAGAAATGGATATG
Keap1 F	CCCATG GAAAGGCTTATTGAGTTC	Keap1 R	GAAGTGCATGTAGATATACTCCC

Table S2. PCR conditions for genotyping, Related to Experimental Procedures

Reaction for *Nrf2*$^{-/-}$

Step #	Temp °C	Time	Notes
1	94	3 min	
2	94	30 sec	
3	56	30 sec	
4	72	30 sec	Repeat Steps 2-4 for 35 cycles
5	72	6 min	Hold

Product Size ---------- ---*NRF2-Tg*: 237 bp, Wt: 300 bp

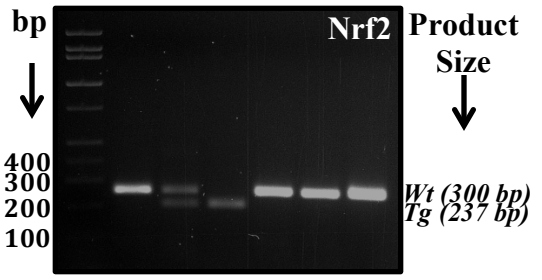

Reaction for *Cre* transgenic allele

Step #	Temp °C	Time	Notes
1	95	2 min	
2	95	30 sec	
3	56	30 sec	
4	72	30 sec	Repeat Steps 2-4 for 40 cycles
5	72	5 min	Hold

Product Size ----------*Cre-Tg*: 247 bp

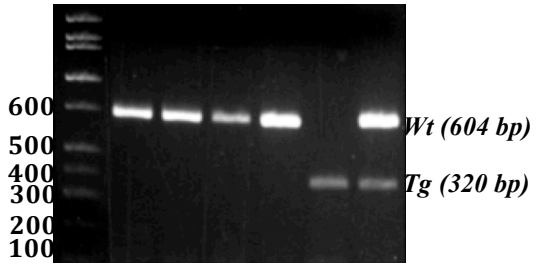

Reaction for *Notch Mutant*

Step #	Temp °C	Time	Notes
	94	2 min	
2	94	20 sec	
3	65	15 sec	Increment: 0.5°C
4	68	10 sec	Repeat Steps 2-4 for 10 cycles
5	94	15 sec	
6	60	15 sec	
7	72	10 sec	Repeat Steps 5-7 for 28 cycles
8	72	1 min	
9	4	-	Hold

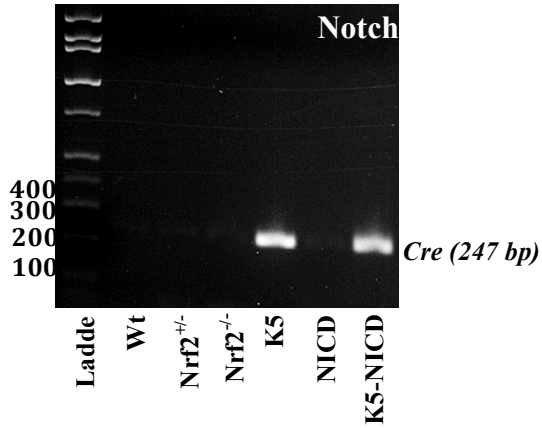

Reaction for *Notch Wt*

Step #	Temp °C	Time	Notes
1	94	2 min	
2	94	20 sec	
3	55	15 sec	
4	68	45 sec	Repeat Steps 2-4 for 10 cycles
5	94	15 sec	
6	55	15 sec	
7	72	45 sec	Repeat Steps 5-7 for 35 cycles
8	72	1 min	
9	4	-	Hold

Product Size ---------- *Notch-Tg*: 320 bp, Wt: 604 bp

Reaction for *Keap1*$^{fl/fl}$

Step #	Temp °C	Time	Notes
1	95	1 min	
2	95	30 sec	
3	68.5	30 sec	
4	72	30 sec	Repeat Steps 2-4 for 35 cycles
5	72	1 min	
6	4	-	Hold

Table S3. List of antibodies for FACS, IF, IHC and WB, Related to Experimental Procedures

Antibody	Raised in	Dilution	Application	Company
Trop2	Goat	1:200	FACS	R and D systems, MN
ITGA6-PE	Rat	1:200	FACS	Abcam, Cambridge, MA
CD44	Rat	1:200	FACS	BD Biosciences
CD166	Goat	1:200	FACS	R and D systems, MN
K5	Rabbit	1:200-400	IF	Covance, Princeton, NJ
K8	Chicken	1: 50	IF	Novus Biologicals, Littleton, CO
Troma for K8	Rat	1: 100	IF	DSHB
Activated Notch	Rabbit	1: 100	IF, WB	Abcam, Cambridge, MA
BrdU	Rat	1: 500	IF	Abcam, Cambridge, MA
βTubulin-acetylated	Mouse	1: 500	IF	Sigma, St. Louis, MO
PIgR	Goat	1: 100	IF	R and D systems, MN
CC10	Goat	1:200	IF	Santa Cruz Biotech, CA
Jagged 1	Rabbit	1:100	IF, WB	Gift from Dr. Gerry Weinmaster
Delta 1	Rabbit	1:100	IF, WB	Gift from Dr. Gerry Weinmaster
Notch-act	Rabbit	1:100	IF	Cell Signaling
p63	Mouse	1:100	IF	Santa Cruz Biotech, CA.
Nrf2	Rabbit	1:100	IHC, WB	Santa Cruz Biotech, CA.
Nqo1	Mouse	1:100	IHC, WB	Cell Signalling
Keap1	Rabbit	1:100	WB	Abcam, Cambridge, MA
Hey1	Rabbit	1:100	IHC, WB	Abcam, Cambridge, MA
HeyL	Rabbit	1:100	IHC, WB	Abcam, Cambridge, MA
Hes1	Rabbit	1:100	IF, WB	Abcam, Cambridge, MA
Ngfr	Rabbit	1:100	IF	Santa Cruz Biotech, CA.
aPKC	Rabbit	1:100	IF	Abcam, Cambridge, MA
γ-Tubulin	Mouse	1:400	IF	Sigma
Actin	Rabbit	1:1000	WB	Cell Signaling
Lactoferrin	Rabbit	1:100	IF	Upstate
Muc5AC	Mouse	1:50	IF	Neomarkers, Freemont, CA

Table S4. Applied Biosystems TaqMan Probes used for qRT-PCR, Related to Experimental Procedures

Mouse Gene	TaqMan Assay	Human Gene	TaqMan Assay
KRT5	Mm001305291_g1	DELTA1	Hs00194509_m1
KRT14	Mm00516876_m1	ITGA6	Hs01041011_m1
TRP63	Mm00495788_m1	JAG1	Hs01070032_m1
Ngfr	Mm01309638_m1	KEAP1	Hs00202227_m1
DELTA1	Mm01279269_m1	KRT5	Hs00361185_m1
HES1	Mm00803077_m1	NOTCH1	Hs01062014_m1
HEY1	Mm00468865_m1	NOTCH2	Hs01050702_m1
JAG1	Mm00496902_m1	NQO1	Hs02512143_s1
JAG2	Mm01325629_m1	NRF2	Hs00975961_g1
NOTCH1	Mm00435249_m1	HES1	Hs00172878_m1
NOTCH2	Mm01342805_m1	HEY1	Hs01114113_m1
NOTCH3	Mm01345646_m1	KRT14	Hs00265033_m1
NFE2L2 (NRF2)	Mm00477784_m1		
NQO1	Mm01253561_m1		
KEAP1	Mm00497268_m1		
SCGB1A1	Mm0042046_m1		
FOXJ1	Mm01267279_m1		

Supplemental Experimental Procedures

Mice

Mouse strains were described previously (Blanpain et al., 2006; McDonald et al., 2010) and were interbred onto the same genetic background (C57BL/6) and genotyped **(Table S1, 2)**. C57BL/6 wild-type (Wt), and *Gt(ROSA)26Sor*$^{tm1(Notch1)Dam}$/J, (008159) mouse strain (annotated Rosa$^{NICD)}$ were purchased from The Jackson Laboratory (Bar Harbor, Maine) (Blanpain et al., 2006). Transgenic C57BL/6 K5-CrePR1 mice were kindly provided by Dr. Stephen Malkoski, University of Colorado Denver Health Sciences Center, Aurora CO, USA (Malkoski et al., 2010). C57BL/6 Nrf2$^{-/-}$ mice were provided by Dr. William McBride from UCLA, CA, USA (McDonald et al., 2010). Keap1$^{fl/fl}$ mice were obtained from Dr. Kupiec-Weglinski with kind permission from Dr. Yamamoto who generated the transgenic mice (Ke et al., 2013). All mice were housed, bred and maintained in a conventional pathogen-free facility at the Division of Laboratory Animal Medicine (DLAM) at UCLA. 6–8-week old Wt and age matched transgenic mice were used for all experiments and were performed in accordance with the guidelines outlined by the DLAM Committee on Animal Care.

Human Tissue

Large airways from normal human patients were obtained from the National Disease Research Interchange Human Tissue Procurement Project or from discarded large airway tissues from normal lung donors at the time of lung transplantation. Human tissues were procured under Institutional Review Board–approved protocols at UCLA.

Fluorescence-Activated Cell Sorting and *In Vitro* Tracheosphere Culture and Treatment

Mouse/Human ABSCs were isolated as reported previously by our laboratory (Hegab et al., 2012b; Hegab et al., 2011). Briefly, tracheas were cut into pieces and incubated or 30 minutes in 16 U/ml dispase (BD Biosciences, Bedford, MA) at room temperature (RT), followed by treatment for 20 minutes in 0.5 mg/ml DNase. Digestion was stopped by addition of DMEM with 5% FBS. Epithelium was peeled off with forceps and incubated in 0.1% trypsin, 1.6 mM EDTA, 20 minutes at 37°C, followed by gentle pipetting and passage through a 40 μm cell strainer to get to a single cell suspension. Total epithelial cells were stained for TROP-2 and ITGA6 for mouse, and CD44 and CD166 for human by incubation with the antibodies in 2% BSA in PBS for 15 minutes at RT followed by washing and incubation with secondary antibodies (see **Table S3** for antibodies used). Sorting was performed using a FACS Aria system, and the data were analyzed using the FACS Diva software (BD Biosciences). Human and Mouse ABSCs *in vitro* tracheosphere assays were performed as reported (Rock et al., 2011; Rock et al., 2009) and previously reported by our laboratory (Hegab et al., 2012b; Hegab et al., 2011).

In Vitro Tracheosphere Culture and Treatment

Tracheosphere culture of human and mouse ABSCs was performed as describe previously health (Rock et al., 2009; Hegab et al., 2011; Hegab et al., 2012a; Hegab et al., 2012b). Briefly FACS-sorted cells were resuspended in mouse tracheal epithelial cells (MTEC)/Plus media, and mixed with growth factor-reduced matrigel (1:1) (BD Biosciences) and then 200 μl/cm pipetted into a 24 well 0.4 μm transwell insert (Falcon). MTEC/Plus (500 μl) was added to the lower chamber and changed every other day. Cultures were maintained at 37°C, 5% CO_2. On day 7, MTEC/Serum Free medium was placed in the lower chamber and changed every other day. The number and diameter of spheres formed per insert was counted on day 7 using an inverted microscope. After 14 days in culture,

spheres were embedded in Histogel (Fisher Scientific, Pittsburgh) and then in paraffin. For 2D cultures the freshly sorted cells were plated onto type I/III collagen-coated transwells and kept submerged in MTEC/Plus media. Media was changed on alternate days for 6 days. ABSCs were treated with the indicated concentrations of oxidants like hydrogen peroxide (H_2O_2) and paraquat, while NAC (N-acetyl-cysteine) and glutathione were used as antioxidants for 14days in tracheospheres cultures. Similarly NOX/DUOX inhibitors apocynin (APO) and diphenylene iodonium (DPI) (Sigma) were used. The gamma secretase inhibitor DBZ ((S,S)-2-[2-(3,5-Difluorophenyl)acetylamino]-N-(5-methyl-6-oxo-6,7-dihydro-5H-dibenzo[b,d]azepin-7-yl)propionamide) (Calbiochem-Millipore, USA) was used at a concentration of 1-20 μM for Notch inhibition and Nrf2 activator Sulforaphane (SFN) (LKT Laboratories Inc, MN, USA) was used at a concentrations of 5-20 μM.

Measurement of Endogenous Reactive Oxygen Species (ROS) Production by Mouse and Human ABSCs

In vivo ROS production was measured by intra-tracheal administration of DHE (Hydroethidine) (10 μl of 20 μM for 30 minutes) (Invitrogen Molecular Probes). Briefly 6-8 week old mice were anesthetized with isoflurane vaporized in a 3:1 mixture of O_2 and air and placed supine while anesthesia was maintained intra-tracheal administration was performed. Tracheas were dissected at 48 hpi and quickly embedded in OCT and sectioned (4 μm) and counterstained with hoechst and mounted with Vectashield (Vector Laboratories, Inc.). Samples were immediately analyzed. Fluorescent intensity was measured using Image J software. Set measurement option was checked for “Area” and “integrated density” followed by selecting the area to be analyzed and fluorescence

integrated density was measured. Fluorescence intensity of approximately 200 nuclei were scored and analyzed (n=6).

ROS production was measured in pure ABSC populations using three ROS-sensitive dyes namely H_2DCFDA (2′ ,7′ –dichloro-dihydrofluorescein diacetate), DHE and Mitosox, (Molecular probe, Invitogen). H_2DCFDA is proposed to react with peroxy products and peroxyl radicals and not with singlet oxygen directly, but singlet oxygen rapidly forms peroxyradicals and thus can indirectly contribute to the formation of DCF (dichloro-dihydrofluorescein). For the measurement of endogenous ROS levels in ABSCs cells, mouse and human ABSCs were labeled with 5 μM of H_2DCFDA, for 30 minutes at 37°C, 5 μM of DHE (cellular superoxide) for 30 minutes or 1 μM Mitosox (mitochondria superoxide) for 20 minutes at 37^{o}C, and then washed three times with PBS. 200 ng/ml DAPI (4',6'-diamidino-2-phenylindole) was added to exclude dead cells and immediately measured by LSRII flow cytometer. H_2DCFDA was used for ROS-based sorting using a FACS Aria cell sorter (BD Biosciences) for the collection of live, DAPI-negative cells with either high ROS (top 20%) or low ROS (bottom 20%) levels (Le Belle et al., 2011; Chuikov et al., 2010). Sorting gates were set by side and forward scatter to eliminate dead and aggregated cells and by positive controls (treated with 100 μM H_2O_2) and negative controls (no exposure to ROS dyes and/or DAPI) cell samples. Cells were collected in MTEC/Plus culture media and cultured immediately in the tracheosphere assay or frozen for RNA extraction.

Immunostaining

Immunostaining was performed as described (Hegab et al., 2011; Hegab et al., 2012a; Hegab et al., 2012b; Ooi et al., 2010; Bisht et al., 2008). Details of the antibodies used are listed in **Table S3**. Briefly mouse tracheas were fixed and longitudinally embedded in paraffin blocks. Tracheospheres

and 2D cultures were fixed in 4% paraformaldehyde, washed and embedded in Histogel and then paraffin embedded and sectioned (5 μm thickness). Immunostaining was done after citrate buffer-mediated antigen retrieval followed by permeabilization with 0.3% Triton X-100 in Dako protein blocking buffer (Dako, North America Inc., USA) for at least 30 minutes at room temperature (RT). Sections were incubated with primary antibodies **(Table S3)**, diluted in blocking solution, overnight at 4°C. After washing, sections were incubated with secondary antibodies for 2–4 hr at RT or overnight at 4°C and then washed and counterstained with DAPI (Vector labs - Burlingame, CA) and analyzed by fluorescent microscopy with a LSM 780 Zeiss confocal microscope (Carl Zeiss, Jena, Germany).

Histology, IHC and ICC

Histological and IHC analyses were performed as described previously (Lawson et al., 2010). For preparation of cytospins, mouse tracheal epithelium were isolated and FACS sorted into basal/stem, and luminal/differentiated cell fractions. Cytospins were fixed with cold acetone (4°C) for 2 min and washed with 1 × PBS. Sections and cytospins were stained with H&E or the antibodies listed in **Table S3**.

Senescence assay

β-Gal staining was performed using senescence-galactosidase staining kit as per the company protocol (Biovision Inc.). Briefly, 10,000 Wt and $Nrf2^{-/-}$ ABSCs were plated in 35mm collagen coated glass bottomed plates, grown for 24 hr and washed with PBS, fixed, and stained with staining solution overnight at 37°C and imaged (Debacq-Chainiaux et al., 2009).

Quantification of γ-tubulin localization and spindle orientation

Late metaphase and anaphase spindles were used for quantification. Spindles that were oriented at 90 ± 30° to the basement membrane were classed as perpendicular; those that were oriented at 0 ± 30° were classed as parallel. Centrioles orientation was determined by the localization of γ-tubulin staining. Image J software was used to measure the angles between the basement membrane and the spindles (Lechler et al., 2005). Radial histograms were constructed using the R software version 3.0.2 (www.r-project.org). They were constructed to quantify the frequency of different fractions of division angles. The 'circular' package and "rose.diag" function was used for the general structure of the graphs.

Cell Cycle Analysis and ROS Flux Measurement

The FUCCI indicator employs a Cdt1-RFP (G1-S reagent) and a geminin-GFP (G2/M reagent), which mark different phase of the cell cycle. In the G1 phase of the cell cycle, only Cdt1 tagged with RFP can be visualized, thus identifying cells in the G1 phase with red fluorescent nuclei. In the S, G2, and M phases, Cdt1 is gradually degraded and only geminin-tagged with GFP remains, thus identifying cells in these phases with green fluorescent nuclei. During the G1/S transition both proteins are present in the cells, allowing GFP and RFP fluorescence to be observed as yellow fluorescence. ABSC transduction with FUCCI was performed according to manufacturer instructions (Invitrogen) (Sakaue-Sawano et al., 2008). Briefly, ABSCs (5×10^4) were plated onto collagen coated coverslips and allowed to attach and grow, followed by addition of Premo^{TM} (component A + B) reagent and incubate overnight at 37°C. Addition of Bacmam enhancer activates efficiency. Live cells were stained with ROS dye (CellROX Deep Red emits in far red) and using a LSM 780 Zeiss confocal microscope. Stained cells were counted and the results were expressed as

percentage of the number of cells in each cell cycle phase (G1, G1-G1/S initiation, G1/S and S/G2/M). The ROS levels in each cell (n=300/condition) were quantified from 3D-merged images (Chuikov et al., 2010; Raj et al., 2011; Le Belle et al., 2011). .

Transmission Electron Microscopy (TEM)

The dissected tracheas were fixed with 2% glutaraldehyde and 2% paraformaldehyde in 0.1 M PBS, pH 7.4, for 2 hr at RT, followed by overnight incubation at 4^{o}C. Tissues were then treated with 0.5% of tannic acid for an hr at RT, followed by wash with PBS buffer (5 times) and postfixed in a solution of 1% OsO_4 in PBS, pH 7.2–7.4. The samples were then washed with Na acetate buffer, pH 5.5 (4 times), block-stained in 0.5% uranyl acetate for 12 hr at 4^{o}C.

The samples were dehydrated in graded ethanol 10 minutes each, passed through propylene oxide, and infiltrated in mixtures of Epon 812 and propylene oxide 1:1 and then 2:1 for 2 hrs each and then infiltrated in pure Epon 812 overnight. Upon embedding and curing was done sections of 60 nm thickness were cut on an ultramicrotome (RMC MTX). The sections were deposited carefully on single-hole grids coated with Formvar and carbon and double-stained in aqueous solutions of 8% uranyl acetate for 25 min at 60°C and lead citrate for 3 minutes at RT. Thin sections subsequently were examined with a 100CX JEOL electron microscope.

Transfection and Immunoblot Analyses

Human and mouse ABSCs were transfected with Nrf2 specific siRNA (Dharmacon-Thermo Scientific) using Lipofectamine RNAi-MAX Transfection Reagent (Invitrogen) and pBOS-ZEDN1 (constitutive active Notch, N^{act}) (Hicks et al., 2000), plasmids were transfected with Lipofectamine 2000 (Invitrogen) according to the manufacturer's protocols. Cells were lysed in RIPA-I lysis buffer,

which contained a protease inhibitor cocktail (Roche, USA). Protein concentrations were estimated using the BCA method. An equal volume of 2xSDS sample buffer was added and the samples were denatured by boiling for 5 minutes. Samples were applied to SDS-PAGE and transferred to an Immobilon PVDF membrane (Millipore, USA). The membranes were blocked with Tris-bufferred saline with 0.05% Tween 20 and 5% skimmed milk and then treated with primary antibodies. The preparative membranes were incubated with appropriate secondary antibodies conjugated to horseradish peroxidase (Invitrogen). The immune-complexes were visualized with the ECL kit (GE-Healthcare, USA) (Ooi et al., 2010; Bisht et al. 2007).

Genetic modification of mABSC isolated from Keap1$^{fl/fl}$ mice

Ad5CMV Cre-eGFP (Ad.GFP) were purchased from gene transfer vector core. Ad.GFP transduction of mABSc was performed as described (Treacy et al., 2012). Briefly, freshly sorted mABSCs were seeded in 6 well plates at a density of 100,000 cells/well in 2 ml of MTEC plus medium for overnight. Medium was then removed and Ad.GFP was added at a multiplicity of infection (MOI) of 100 to the cells followed by spin centrifugation for 90 min at 2,000 g at 37^{o}C. The medium was removed and fresh medium were added to the cells. Light and fluorescent microscopy was performed 24 hr after transduction. Cells were detached with 0.25% trypsin/1 mM EDTA at 37^{o}C and centrifuged at 400 g for 5 mins. After washing, cell pellets were resuspended in FACS buffer. The cells expressing GFP was resorted using a FACS Aria (BD Biosciences) and were subjected to tracheosphere culture.

Reverse Transcriptase Real-time quantitative PCR (qPCR)

RNA was isolated using RNeasy micro kit (Qiagen) according to the manufacturer's protocol. Total

RNA was DNase-treated with RQ1 RNase-Free DNase (Promega). Reverse transcription was performed with SuperScript II First Strand Kit (Invitrogen). qPCR was performed with the Taqman PCR Master Mix (Applied Biosystems) on an Applied Biosystems StepOne-plus Real-Time PCR System. Primer sequences used are described in **Table S4**. For analysis, the Δ*C*T method was applied with GAPDH as an endogenous control. Relative gene expression is presented as a ratio of target gene to reference control (Hegab et al., 2011; Ooi et al., 2010).

Nuclear Protein Extraction and Electrophoretic Mobility Shift Assay (EMSA)

To confirm transcriptional activation of Notch by Nrf2 we used EMSA. Prior to preparing nuclear extracts, bronchoalveolar tissues were incubated with 50 μM sulforaphane overnight at 37°C to activate Nrf2. Briefly, nuclear protein extracts were prepared using NE-PER extraction reagents (Thermo Scientific) according to the manufacturer's instructions. The sequences used to generate probes containing the Notch1 ARE were as per previously published (Wakabayashi et al., 2002). Probes were biotinylated using a Biotin 3′ End labeling Kit (Thermo Scientific) according to the manufacturer's instructions. EMSAs were performed by incubating protein (3.5 μg) in binding buffer (10 mM HEPES, 60 mM KCl, 0.5 mM EDTA, 4 % Ficoll, 1 mM DTT, 1 mM PMSF, and 5 μg of Herring sperm DNA) for 20 minutes at 4°C, prior to the addition of biotinylated probe. Supershift experiments were performed by incubating protein with ChIP grade anti-Nrf2 antibody (Epitomics or IgG control) in binding buffer 1 hr prior to the addition of probe. Binding reactions were subjected to electrophoresis on a 5 % polyacrylamide gel with 0.5 X TBE, transferred to a nylon membrane, and cross-linked at 120 mJ/cm^2, using a UV-light crosslinker. The biotinylated DNA was detected using the Chemiluminescent Nucleic Acid Detection Module (Thermo Scientific).

Proliferation Assay

For studies of self-renewal and proliferation *in vivo*, 5-bromo-2'-deoxyuridine (BrdU, Sigma-Aldrich) was injected intra-peritoneally (50mg kg^{-1}) to label cells in S-phase following standard procedure. The BrdU injection scheme is shown in Figure S2A. BrdU+/DAPI+ cells were counted in 10 μm projections of ten confocal optical sections at 20 x 10X magnification per trachea.

Cell proliferation *in vitro* was assessed by 5-ethynyl-2′ -deoxyuridine (EdU) incorporation using the Click-iT EdU Alexa Fluor-488 cell proliferation assay kit (Invitrogen, Carlsbad, CA). Cells were cultured as submerged monolayer at 20,000 cells per well in growth medium and were given different treatments for specific time points (as indicated in each experiment). For EdU incorporation, EdU solution was added to the medium for the last 5 hrs of the incubation period and processed as per the manufacturer's protocol. At least 5000 cells in 10 random high power fields were counted per experiment.

The percentage of dividing epithelial cells (BrdU+/DAPI+) was calculated by analyzing serial sections from 24, 48 and 72 hpi tracheal samples. Using NIH ImageJ software, the cell counting of DAPI+ cells and BrdU+ cells was done and manual counting was used to crosscheck the data. The threshold of the DAPI channel image was selected to B & W, with dark background, binary and watershed channels selected and then particle number analyzed (0-∞; 0.00–1.00, show outline, display result) to give the number of DAPI+ cells and same was done with the BrdU channel. Manual counting was done to crosscheck BrdU+ cell numbers. Notch inhibition was achieved by intraperitoneally administration of 30 μmol/kg DBZ or vehicle daily for 5 days (VanDussen et al., 2012).

Supplemental References

Bisht, B., and Dey, C.S., (2008). Focal Adhesion Kinase contributes to insulin-induced actin reorganization into a mesj harboring glucose transporter-4 in insulin resistant skeletal muscle cells. BMC Cell Biol *4*, 9:48.

Bisht, B., Goel, H.L., and Dey, C.S. (2007). Focal adhesion kinase regulates insulin resistance in skeletal muscle. Diabetologia *50*, 1058-1069.

Chuikov, S., Levi, B.P., Smith, M.L., and Morrison, S.J. (2010). Prdm16 promotes stem cell maintenance in multiple tissues, partly by regulating oxidative stress. Nat Cell Biol *12*, 999-1006.

Debacq-Chainiaux, F., Erusalimsky, J.D., Campisi, J., and Toussaint, O. (2009). Protocols to detect senescence-associated beta-galactosidase (SA-βgal) activity, a biomarker of senescent cells in culture and *in vivo.* Nat Protoc *4*, 1798-1806.

Hegab, A.E., Ha, V.L., Attiga, Y.S., Nickerson, D.W., and Gomperts, B.N. (2012a). Isolation of basal cells and submucosal gland duct cells from mouse trachea. J Vis Exp 10.3791/3731, e3731.

SUPPLEMENTAL INFORMATION

Hegab, A.E., Ha, V.L., Darmawan, D.O., Gilbert, J.L., Ooi, A.T., Attiga, Y.S., Bisht, B., Nickerson, D.W., and Gomperts, B.N. (2012b). Isolation and in vitro characterization of Basal and submucosal gland duct stem/progenitor cells from human proximal airways. Stem Cells Transl Med *1*, 719-724.

Hegab, A.E., Ha, V.L., Gilbert, J.L., Zhang, K.X., Malkoski, S.P., Chon, A.T., Darmawan, D.O., Bisht, B., Ooi, A.T., Pellegrini, M.*, et al.* (2011). Novel stem/progenitor cell population from murine tracheal submucosal gland ducts with multipotent regenerative potential. Stem Cells *29*, 1283-1293.

Hicks, C., Johnston, S.H., diSibio, G., Collazo, A., Vogt, T.F., and Weinmaster, G. (2000). Fringe differentially modulates Jagged1 and Delta1 signalling through Notch1 and Notch2. Nat Cell Biol *2*, 515-520.

Lawson, D.A., Zong, Y., Memarzadeh, S., Xin, L., Huang, J., and Witte, O.N. (2010). Basal epithelial stem cells are efficient targets for prostate cancer initiation. Proc Natl Acad Sci U S A *107*, 2610-2615.

Le Belle, J.E., Orozco, N.M., Paucar, A.A., Saxe, J.P., Mottahedeh, J., Pyle, A.D., Wu, H., and Kornblum, H.I. (2011). Proliferative neural stem cells have high endogenous ROS levels that regulate self-renewal and neurogenesis in a PI3K/Akt-dependant manner. Cell Stem Cell *8*, 59-71.

Lechler, T., and Fuchs, E. (2005). Asymmetric cell divisions promote stratification and differentiation of mammalian skin. Nature *437*, 275-280.

Ooi, A.T., Mah, V., Nickerson, D.W., Gilbert, J.L., Ha,V.L., Hegab, A.E., Horvath, S., Alavi, M., Maresh., E.L.*, et al.* (2010). Presence of a putative tumor-initiating progenitor cell population predicts poor prognosis in smokers with non-small cell lung cancer. Cancer Res *15*, 6639-6648.

Raj, L., Ide, T., Gurkar, A.U., Foley, M., Schenone, M., Li, X., Tolliday, N.J., Golub, T.R., Carr, S.A., Shamji, A.F.*, et al.* (2011). Selective killing of cancer cells by a small molecule targeting the stress response to ROS. Nature *475*, 231-234.

Rock, J.R., Onaitis, M.W., Rawlins, E.L., Lu, Y., Clark, C.P., Xue, Y., Randell, S.H., and Hogan, B.L. (2009). Basal cells as stem cells of the mouse trachea and human airway epithelium. Proc Natl Acad Sci U S A *106*, 12771-12775.

Sakaue-Sawano, A., Kurokawa, H., Morimura, T., Hanyu, A., Hama, H., Osawa, H., Kashiwagi, S., Fukami, K., Miyata, T., Miyoshi, H.*, et al.* (2008). Visualizing spatiotemporal dynamics of multicellular cell-cycle progression. Cell *132*, 487-498.

Treacy, O., Ryan, A.E., Heinzl, T., O'Flynn, L., Cregg, M., Wilk, M., Odoardi, F., Paul, L., O'Brien1, T., Nosov, M., and Ritter, T. (2012). Adenoviral transduction of mesenchymal stem cells: In Vitro responses and In Vivo immune responses after cell transplantation. PLoS ONE *7*, e42662.

VanDussen, K. L., Carulli, A.J., Keeley, T.M., Patel, S.R., Puthoff, B.J., Magness, S.T., Tran, I.T., Maillard, I., Siebel, C., Kolterud, Å., *et al.* (2012). Notch signaling modulates proliferation and differentiation of intestinal crypt base columnar stem cells. Development *139*, 488-497.

SUPPLEMENTAL INFORMATION

Wakabayashi, N., Shin, S., Slocum, S.L., Agoston, E.S., Wakabayashi, J., Kwak, M.K., Misra, V., Biswal, S., Yamamoto, M., and Kensler, T.W. (2010). Regulation of notch1 signaling by nrf2: implications for tissue regeneration. Sci Signal *3*, ra52.